EUROPEAN ORGANIZATION FOR NUCLEAR RESEARCH

MEASUREMENT AND ANALYSIS OF THE $\pi^+\pi^+$ SYSTEM PRODUCED AT SMALL MOMENTUM TRANSFER IN THE REACTION $\pi^+p \to \pi^+\pi^+n$ AT 12.5 GeV

W. Hoogland and S. Peters

Zeeman Laboratorium, University of Amsterdam*),
Amsterdam, The Netherlands

G. Grayer**), B. Hyams and P. Weilhammer

CERN, Geneva, Switzerland

W. Blum, H. Dietl, G. Hentschel, W. Koch***), E. Lorenz,
G. Lütjens, G. Lutz, W. Männer, R. Richter and U. Stierlin

Max-Planck-Institut für Physik und Astrophysik,
Munich, Germany

ABSTRACT

From a wire chamber experiment 45,452 events were obtained from the reaction $\pi^+p \to \pi^+\pi^+n$. The I = 2 phase shifts were determined in the $\pi^+\pi^+$ mass region 0.3-1.5 GeV. An amplitude analysis was performed. The results are compared with some theoretical predictions.

Geneva - 21 March 1977

(Submitted to Nuclear Physics)

---

*) The work in Amsterdam is part of the joint research programmes of FOM and ZWO.

**) Now at Rutherford Laboratory, Chilton, Didcot, England.

***) Now at DESY, Hamburg, Germany.

1. INTRODUCTION

In this paper we report results of the analysis of the reaction

$$\pi^+ p \to \pi^+\pi^+ n \qquad (1)$$

at 12.5 GeV incident beam momentum.

The data are part of the experimental programme accomplished with the CERN-Munich spectrometer at the CERN PS[1]. The 45,452 events of reaction (1) with a forward produced $\pi^+\pi^+$ system are used in this analysis. This is a factor of three increase in statistics compared with the data used in a previous analysis of this reaction by our group[2].

The present analysis, using the larger data sample, confirms the results given in Ref. 2. Because of the improved statistical significance of our data we are able to determine the on-mass-shell I = 2 s-wave and d-wave phase shifts in smaller intervals of the $\pi\pi$ invariant mass. Moreover, we are able to do a more detailed analysis of the production mechanism of the forward produced $\pi\pi$ system, which appears to have strikingly similar features to those of the $\pi^+\pi^-$ system in the reaction

$$\pi^- p \to \pi^-\pi^+ n \ . \qquad (2)$$

2. EXPERIMENTAL DETAILS

A detailed description of the apparatus, the data processing, and the methods used to extract the spherical harmonic moments of the $\pi\pi$ angular distribution, has been given in Ref. 1. The data of reaction (1) were obtained in several runs extended over three years. Extensive cross-checks have been made between the various runs to ensure that no systematic discrepancies exist. An unseparated positive beam of 12.5 GeV momentum impinged on a 52 cm long liquid hydrogen target. Threshold Čerenkov counters in the beam line were used to select the incoming π^+ particles, representing about 10% of the total beam flux. It was checked that, in all runs, proton breakthrough was less than 1% of the π^+ flux. Reaction (1) was selected by triggering on the incoming π^+ and on two charged particles emerging from the H_2 target in the forward direction. The particle trajectories were measured before and after a large spectrometer magnet, with a total bending power of 2 T•m, thus allowing the momentum of the particle to be determined with a precision of better than 0.5%. Background of events with additional π^0's was suppressed by using the information of a set of anticounters, shielding the target and covering the front end of the magnet and the magnet gap faces.

In Fig. 1 we show the missing-mass spectrum of events with and without the condition that none of these anticounters has fired. Our working sample consisted of events with a missing mass smaller than 1.2 GeV. We estimate that the background

from events with additional π^0's in this sample is (2 ± 0.5%), using additional calibration measurements. The missing-mass resolution amounts to about ±80 MeV. It is dominated by the momentum resolution of the beam particle and of the faster of the two outgoing π^+ particles. The resolution of the $\pi^+\pi^+$ invariant mass is estimated in Ref. 1 to be approximately ±7 MeV for $M_{\pi\pi}$ = 1000 MeV.

The absolute cross-section for our total data sample amounts to

$$\sigma(1 \text{ produced event}) = 0.257 \pm 0.018 \text{ nb} . \qquad (3)$$

This value has been calculated in a similar way to that described in Ref. 1 and takes into account all known systematic losses. The error in formula (3) is almost exclusively due to the uncertainties in estimating the various correction factors. The observed total cross-sections for the individual runs agree within the quoted error.

3. ANGULAR DISTRIBUTIONS

In order to correct for the geometrical acceptance of our apparatus, a set of Monte Carlo data have been generated for fixed values of $M_{\pi\pi}$, the $\pi^+\pi^+$ invariant mass, and t, the squared four-momentum transfer to the nucleon, and with an isotropic angular distribution of the π^+ in the $\pi^+\pi^+$ rest frame. Because of the slightly different experimental conditions of the individual runs, these Monte Carlo calculations had to be repeated for each run. The weighted average of the Monte Carlo data was used to calculate the acceptance-corrected results from the total data sample. Since the acceptance of the apparatus drops rapidly for increasing $M_{\pi\pi}$ the analysis was restricted to an upper limit of 1.5 GeV, above which the average acceptance becomes less than 10%. In Fig. 2 the observed and acceptance-corrected mass spectra are shown for events in the interval $-t_{min} < -t < 0.2$ GeV^2.

The spherical harmonic moments of the $\pi\pi$ angular distribution $\langle \text{Re } Y_\ell^m \rangle$ in the expression for the differential cross-section:

$$\frac{d^4\sigma}{dt dM_{\pi\pi} d\Omega} = \frac{d^2\sigma}{dt dM_{\pi\pi}} \sum_{\ell=0}^{\ell_{max}} \left\{ \langle Y_\ell^0 \rangle Y_\ell^0(\Omega) + 2 \sum_{m=1}^{\ell} \langle \text{Re } Y_\ell^m \rangle \text{ Re } Y_\ell^m(\Omega) \right\} \qquad (4)$$

were determined by a χ^2-method (see Ref. 1). Only even ℓ values contribute for reaction (1) because of the symmetry of the $\pi\pi$ system. The mass dependences of the t-channel spherical harmonics $\langle \text{Re } Y_\ell^m \rangle$ for $\ell \leq 6$ and $m \leq 1$ are shown in Fig. 3, for mass intervals of 20 MeV, integrated over the t-range $-t_{min} < -t < 0.2$ GeV^2. All moments with $m \geq 2$ and also those with $\ell \geq 8$, not shown here, are consistent with zero over the mass range considered. This is also the case for $\langle Y_6^0 \rangle$. The

smallness of the moments with $\ell \geq 6$ indicates that the g-wave contribution is extremely small in this mass range.

In Fig. 4 the t-dependence of the moments up to $\ell = 4$ is shown in both t- and s-channel helicity frames, for values of $M_{\pi\pi}$ in the range 0.75 GeV < $M_{\pi\pi}$ < < 1.25 GeV.

For the same mass interval we show in Fig. 5 the differential cross-section. In the same figure we indicate the differential cross-section for events with a $\pi^+\pi^+$ invariant mass in the range 0.35 < $M_{\pi\pi}$ < 0.75 GeV. The data demonstrate that the slope of the differential cross-section becomes less steep for decreasing invariant mass.

The following expressions for the spherical harmonic moments of the $\pi\pi$ angular distributions are obtained, if one assumes only s- and d-waves to be present, and further assumes (nucleon) spin coherence of the helicity amplitudes[3].

$$N\langle Y_0^0\rangle = \sqrt{\frac{1}{4\pi}}\left\{|S|^2 + |D_0|^2 + \frac{1}{2}\left(|D_1^+|^2 + |D_1^-|^2\right) + \frac{1}{2}\left(|D_2^+|^2 + |D_2^-|^2\right)\right\} \tag{5a}$$

$$N\langle Y_2^0\rangle = 2\sqrt{\frac{1}{4\pi}}\left\{\mathrm{Re}\left(S \cdot D_0\right) + \frac{1}{7}\sqrt{5}|D_0|^2 + \frac{1}{28}\sqrt{5}\left(|D_1^+|^2 + |D_1^-|^2\right) - \frac{1}{14}\sqrt{5}\left(|D_2^+|^2 + |D_2^-|^2\right)\right\} \tag{5b}$$

$$N\langle \mathrm{Re}\, Y_2^1\rangle = \sqrt{\frac{1}{4\pi}}\left\{\mathrm{Re}\left(S \cdot D_1^-\right) + \frac{1}{7}\sqrt{5}\,\mathrm{Re}\left(D_0 \cdot D_1^-\right) + \frac{1}{14}\sqrt{30}\left[\mathrm{Re}\left(D_1^- \cdot D_2^-\right) + \mathrm{Re}\left(D_1^+ \cdot D_2^+\right)\right]\right\} \tag{5c}$$

$$N\langle \mathrm{Re}\, Y_2^2\rangle = \sqrt{\frac{1}{4\pi}}\left\{\mathrm{Re}\left(S \cdot D_2^-\right) - \frac{2}{7}\sqrt{5}\,\mathrm{Re}\left(D_0 \cdot D_2^-\right) - \frac{1}{28}\sqrt{30}\left(|D_1^+|^2 - |D_1^-|^2\right)\right\} \tag{5d}$$

$$N\langle Y_4^0\rangle = 2\sqrt{\frac{1}{4\pi}}\left\{\frac{3}{7}|D_0|^2 - \frac{1}{7}\left(|D_1^+|^2 + |D_1^-|^2\right) + \frac{1}{28}\left(|D_2^+|^2 + |D_2^-|^2\right)\right\} \tag{5e}$$

$$N\langle \mathrm{Re}\, Y_4^1\rangle = \sqrt{\frac{1}{4\pi}}\left\{\frac{1}{7}\sqrt{30}\,\mathrm{Re}\left(D_0 \cdot D_1^-\right) - \frac{1}{14}\sqrt{5}\left[\mathrm{Re}\left(D_1^- \cdot D_2^-\right) + \mathrm{Re}\left(D_1^+ \cdot D_2^+\right)\right]\right\} \tag{5f}$$

$$N\langle \mathrm{Re}\, Y_4^2\rangle = \sqrt{\frac{1}{4\pi}}\left\{\frac{1}{7}\sqrt{15}\,\mathrm{Re}\left(D_0 \cdot D_2^-\right) - \frac{1}{14}\sqrt{10}\left(|D_1^+|^2 - |D_1^-|^2\right)\right\} \tag{5g}$$

$$N\langle \mathrm{Re}\, Y_4^3\rangle = \sqrt{\frac{1}{4\pi}}\left\{\frac{1}{2}\sqrt{\frac{5}{7}}\left[\mathrm{Re}\left(D_1^- \cdot D_2^-\right) - \mathrm{Re}\left(D_1^+ \cdot D_2^+\right)\right]\right\} \tag{5h}$$

$$N\langle \mathrm{Re}\, Y_4^4\rangle = \sqrt{\frac{1}{4\pi}}\left\{\frac{1}{4}\sqrt{\frac{10}{7}}\left(|D_2^-|^2 - |D_2^+|^2\right)\right\} \tag{5i}$$

with $N = d^2\sigma/dt dM_{\pi\pi}$.

Here S and D_0, D_1^+, D_1^-, D_2^+, D_2^- refer to amplitudes for production of a dipion with L = 0 and L = 2, respectively. The helicity 0, 1, or 2 of the dipion is indicated by the subscript. The superscripts + and - indicate combinations of helicity states corresponding to natural and unnatural parity exchange, respectively:

$$D_1^\pm = D_1 \pm D_{-1}\,, \qquad D_2^\pm = D_2 \mp D_{-2}\,. \tag{6}$$

The qualitative remarks made in our previous paper[2] on the basis of a comparison of the moment equations (5) with the distributions shown in Figs. 2-5 are still valid for this analysis with its larger statistics. In particular, we mention:

i) the absence of any indication of a resonance structure for $M_{\pi\pi} < 1.5$ GeV, as follows from the smooth mass dependence of both the cross-section and the moments;

ii) the presence of a d-wave component in the $\pi\pi$ amplitudes from about 0.5 GeV upwards, as indicated by the significantly non-zero values of $\langle Y_2^0 \rangle$ [the corresponding $\langle Y_4^0 \rangle$ values being small, however, the relative contribution to the cross-section is concluded to be small];

iii) the significantly non-zero values of the m = 1 moments, indicating that even at low momentum transfers, where π-exchange is assumed to be dominating, helicity-one d-waves cannot be neglected;

iv) the m = 2 moments being consistent with zero, for momentum transfers $-t < 0.15$ GeV^2;

v) the turnover of the differential cross-section at approximately $-t = m_\pi^2$, which is typical for processes dominated by π-exchange.

It is interesting to compare the t-dependence of the $m \neq 0$ moments with those of the reaction $\pi^- p \to \pi^- \pi^+ n$. Although with much smaller statistics, the $\pi^+\pi^+$ data show a very similar behaviour. In particular, the m = 1 s-channel helicity moments seem to cross zero near $\sqrt{-t} = m_\pi$, similarly to what is observed for the $\pi^+\pi^-$ data. This is a typical feature of absorptive π-exchange models like the Williams model[4]. Such models therefore may also provide a good description of the production mechanism of reaction (1) for low values of -t. It demonstrates that the prescriptions to include absorption are indeed independent of the isotopic spin state of the $\pi\pi$ system. In Section 5 we will discuss this in more detail.

The $\pi^+\pi^-$ spherical harmonics in the f-region indicate that natural parity exchange is dominating for larger values of -t. In the case of the $\pi^+\pi^+$ data it would then follow from Eq. (5) that either $\langle \mathrm{Re}\, Y_4^2 \rangle$ or $\langle \mathrm{Re}\, Y_4^4 \rangle$ is negative. This appears to be in conflict with the observed behaviour of these moments.

4. PHASE-SHIFT ANALYSIS

As in reaction (2) we assume π-exchange to be dominating in the reaction $\pi^+ p \to \pi^+\pi^+ n$ for $-t < 0.15$ GeV^2. Strong evidence for this assumption comes from the shape of the differential cross-section and from the behaviour of the moments of the $\pi^+\pi^+$ angular distribution.

With this assumption, reaction (1) can be used to extract information on the phase shifts of I = 2 elastic $\pi\pi$ scattering. In Ref. 2 two methods were used to determine the s- and d-wave phase shifts, δ_s and δ_d, all higher partial waves being negligible in the mass range considered ($0.5 < M_{\pi\pi} < 1.5$ GeV). The first method (A) was a conventional Chew-Low extrapolation. The m = 0 moments in the t-channel helicity (Jackson) system were extrapolated to the pion pole with a simple polynomial in t. The standard Chew-Low formula was used, modified with Dürr-Pilkuhn form factors for the nucleon vertex. In the second method (B), δ_s and δ_d were obtained by fitting the m = 0 and m = 1 s-channel helicity moments to OPE amplitudes with absorptive corrections. The above analysis has been repeated with the present higher statistics. In the following, we review the basic formulae used in both methods.

(A) The m = 0 t-channel helicity moments with ℓ = 0, 2, 4 are parametrized according to[5)]

$$\frac{d^2\sigma}{dt\,dM_{\pi\pi}} \langle Y_\ell^0 \rangle \propto F(t) \left[-\mu^2 - a_\ell(t - \mu^2) - b_\ell(t - \mu^2)^2\right] S_{\pi\pi} \ . \tag{7}$$

A correct description of the differential cross-section required a quadratic term in expression (7) for ℓ = 0. The results, however, were hardly affected by also allowing b_2 and b_4 to vary in the fit. They were therefore fixed to be $b_2 = b_4 = 0$. F(t) is the Dürr-Pilkuhn form factor:

$$F(t) = \frac{1 + 8.2\ \text{GeV}^{-2}\ Q^2}{1 + 8.2\ \text{GeV}^{-2}\ Q^2(t)} \tag{8}$$

with

$$Q^2(t) = \frac{-t(4m_p^2 - t)}{4m_p^2} \ ,$$

and

$$Q^2 = Q^2(\mu^2) \ ,$$

μ and m_p being the masses of the π-meson and of the proton, respectively. $S_{\pi\pi}$ is a bilinear expression of s-wave and d-wave dipion production amplitudes. These amplitudes follow from Eqs. (5) by neglecting all amplitudes except S and D_0. S and D_0 may be written as

$$\begin{aligned} S &= \gamma\, A_s \frac{1}{\sqrt{t - \mu^2}} \\ D_0 &= \gamma \sqrt{5}\, A_d \frac{1}{\sqrt{t - \mu^2}} \ , \end{aligned} \tag{9}$$

where A_s and A_d contain the s- and d-wave phase shifts through

$$A_{s,d} = e^{i\delta_{s,d}} \sin \delta_{s,d} \tag{10}$$

and

$$\gamma^2 = \frac{M_{\pi\pi}^2}{4\pi\, m_p^2\, p_{lab}^2} \frac{g^2}{4\pi} \frac{8\pi}{q_\pi} . \tag{11}$$

(B) In this method the amplitudes S, D_0, D_1^+, and D_1^- are fitted to the s-channel helicity m = 1 and m = 0 moments for $-t_{min} \leq -t \leq 0.15$ GeV^2. Since all moments with $m \geq 1$ are consistent with zero in this t-range, the helicity-two amplitudes can be neglected. The following amplitudes are used (see for instance Ref. 3):

$$\begin{aligned}
S &= \gamma\, A_s \frac{(-t')^{\frac{1}{2}}}{t - \mu^2} e^{B(t-\mu^2)} \\
D_0 &= \gamma \sqrt{5}\, A_d \frac{(-t')^{\frac{1}{2}}}{t - \mu^2} \left(\frac{1 + 2\mu^2/M_{\pi\pi}}{1 - 4\mu^2/M_{\pi\pi}^2} \right) e^{B(t-\mu^2)} \\
D_1^- &= \gamma \frac{\sqrt{30}}{M_{\pi\pi}} A_d \left\{ \frac{2(-t')}{t - \mu^2} \frac{1}{1 - 4\mu^2/M_{\pi\pi}^2} + c \right\} e^{B(t-\mu^2)} \\
D_1^+ &= -\gamma \frac{\sqrt{30}}{M_{\pi\pi}} A_d\, c\, e^{B(t-\mu^2)}
\end{aligned} \tag{12}$$

with A_s and A_d defined before, and $t' = t - t_{min}$. The absorptive correction c has been assumed to be a real constant. In the pure Williams model c = 1. The $\pi^+\pi^-$ data, however, have shown that c depends on $M_{\pi\pi}$, decreasing for increasing $M_{\pi\pi}$. Therefore c has been taken as a free parameter in our fit together with δ_s, δ_d, and the slope B of the exponential (which here is assumed to be the same for all amplitudes). It appears that the δ_s and δ_d as determined in the fit depend only weakly on c. Fixing c at a value c = 0.5, as was done in our previous analysis, gives almost identical results.

In both methods we have assumed the scattering process to be completely elastic. One might expect this assumption to be wrong for large values of $M_{\pi\pi}$. An indication for the possible presence of inelastic channels leading to a value of the elasticity parameter η of less than one might be seen in the acceptance-corrected invariant mass spectrum. This distribution seems to level off slightly above $M_{\pi\pi}$ = 1.2 GeV. Unfortunately the number of observables in our experiment is too small to obtain a reliable estimate of η, given the strong correlation between δ_s and η and the fact that the errors on $\langle Y_2^0 \rangle$ are too large to make $\langle Y_2^0 \rangle$

a good constraint. We have, nevertheless, tried to perform an amplitude fit (B) with η as a free parameter. To do this, c was fixed for each mass interval. The values of η so obtained were not significantly different from one in the mass range studied in this experiment. δ_s and δ_d were determined in mass bins of 100 MeV in the mass range $0.3 \leq M_{\pi\pi} \leq 1.5$ GeV.

The results are listed in Table 1. For method (B), the listed values are those obtained in a fit with δ_s, δ_d, c, and B as free parameters. All fitted values are shown in Figs. 6 and 7. As stated before, the results obtained with a constant value, c = 0.5, are equal within the errors. Our values of δ_s^2 agree well with solution 1 of the dispersion relation calculations of Basdevant et al.[6]. For δ_d^2, however, there is a disagreement. The observed values are much larger than either of the solutions of Basdevant et al. For both δ_s and δ_d the predicted values of Basdevant et al. are shown in Fig. 6. In the $\pi^+\pi^-$ data a similar discrepancy between observed and predicted values was found for the p-wave phase shifts; however, only at masses below 700 MeV [7]. The disagreement observed for our d-wave phase shifts appears to be much larger and also persists to larger values of $M_{\pi\pi}$.

5. ABSORPTIVE EFFECTS

In the previous section, the s- and d-wave phase shifts were determined by fitting the m = 0 and m = 1 s-channel helicity moments for ℓ = 0, 2, and 4, to π-exchange amplitudes with absorptive corrections, closely resembling those of the Williams or Poor Man's Absorption model. The absorptive cut is represented by the real constant c in Eqs. (12). In the original Williams model it is set equal to one, independent of $M_{\pi\pi}$, thus predicting, as the most noticeable feature, the zero-crossing of the m = 1 moments at $t = -\mu^2$.

The $\pi^+\pi^-$ data, however, have shown that c is not independent of $M_{\pi\pi}$, but decreases for increasing mass, indicating that the absorptive effects apparently become less important for higher values of $M_{\pi\pi}$. Our results, as shown in Fig. 7, indicate that a similar behaviour appears to be present in the $\pi^+\pi^+$ data, although the absolute values appear to be smaller than those obtained for the $\pi^+\pi^-$ data, at the same $\pi\pi$ invariant mass. The striking similarity of $\pi^+\pi^+$ and $\pi^+\pi^-$ data is best shown by plotting the ratio $\langle \mathrm{Re}\ Y_2^1\rangle/\langle \mathrm{Re}\ Y_2^0\rangle$, with $\langle \mathrm{Re}\ Y_2^1\rangle$ and $\langle \mathrm{Re}\ Y_2^0\rangle$ determined in the t-channel helicity or Jackson frame and integrated over the t-interval $-t_{min} < -t < 0.15\ \mathrm{GeV}^2$ (Fig. 8). According to Ochs and Wagner[8] this ratio is related to the absorptive cut constant c through

$$\mathrm{Re}\ c_A \approx -\langle \mathrm{Re}\ Y_\ell^1\rangle/\langle \mathrm{Re}\ Y_\ell^0\rangle \sqrt{M_{\pi\pi}/\ell(\ell+1)}\ . \qquad (13)$$

The corresponding values of the $\pi^+\pi^-$ data are shown in the same figure, for comparison. The agreement appears to be remarkably good. The same ratio for the $\ell = 4$ moments, not shown here, also gives good agreement, although the errors here are much larger. From the ratio of the $\ell = 2$ moments, c has been determined according to formula (13). The value c = 0.85 at $M_{\pi\pi} = 0.55$ GeV, as obtained from our amplitude fit, is used for normalization. The results are indicated in Fig. 6. We observe that the values of c, as determined with these two independent methods, agree extremely well. According to our amplitude fit, also the slope parameter B, which accounts for the helicity-independent part of the t-dependence of the helicity amplitudes, depends strongly on $M_{\pi\pi}$. The exponential becomes steeper for higher values of $M_{\pi\pi}$.

In our fit, for both the s- and d-wave amplitudes, the same value of B has been used. Since the s-wave amplitude is the dominant one in our data, we are essentially measuring the exponential slope of the s-wave amplitude. In the paper by Humble[9], the "b-universality" hypothesis, which relates the impact parameter profiles of helicity amplitudes for different values of the net helicity flip, has been modified to describe π-exchange processes. In this modified "b-universality" scheme a simple relation is obtained between the absorptive cut correction c of the previous sections and the slope parameter B;

$$c = \frac{2\Lambda}{\Lambda - B^2} , \qquad (14)$$

where Λ is a normalizing constant. If we assume B to be the same for both s- and d-wave amplitudes, our measured values of B can be inserted in Eq. (14) to relate our measurement of c and B. In Fig. 6 we show the mass dependence of c, calculated for a smooth curve drawn through the measured B values and after normalization of the value c = 0.85 at $M_{\pi\pi} = 0.55$ GeV. Indeed the calculated curve accounts extremely well for the observed mass dependence of c.

REFERENCES

1) G. Grayer, B. Hyams, C. Jones, P. Schlein, P. Weilhammer, W. Blum, H. Dietl, W. Koch, E. Lorenz, G. Lütjens, W. Männer, J. Meissburger, W. Ochs and U. Stierlin, Nuclear Phys. B75, 189 (1974).

2) W. Hoogland, G. Grayer, B. Hyams, C. Jones, P. Weilhammer, W. Blum, H. Dietl, W. Koch, E. Lorenz, G. Lütjens, W. Männer, J. Meissburger and U. Stierlin, Nuclear Phys. B69, 266 (1974).

3) P. Estabrooks, A. Martin, G. Grayer, B. Hyams, C. Jones, P. Weilhammer, W. Blum, H. Dietl, W. Koch, E. Lorenz, G. Lütjens, W. Männer, J. Meissburger and U. Stierlin, Proc. Internat. Conf. on ππ scattering, Tallahassee, 1973 (American Institute of Physics, New York, 1973), p. 37.

4) G.L. Kane and M. Ross, Phys. Rev. 177, 2353 (1969);
P.K. Williams, Phys. Rev. D 1, 1313 (1970);
G.C. Fox, Proc. Conf. on Phenomenology in Particle Physics, Pasadena, 1971 (CalTech, Pasadena, 1971), p. 703.

5) G. Grayer, B. Hyams, C. Jones, P. Schlein, W. Blum, H. Dietl, W. Koch, U. Stierlin and P. Weilhammer, Proc. 3rd Internat. Conf. on Experimental Meson Spectroscopy, Philadelphia, 1972 (American Institute of Physics, New York, 1972), p. 5.

6) J.L. Basdevant, C.D. Froggatt and J.L. Petersen, Proc. 2nd Internat. Conf. on Elementary Particles, Aix-en-Provence, 1973 (J. Phys. 34, Colloque C-1, Suppl. to No. 10), p. 220, and Construction of phenomenological ππ amplitudes, Preprint, Laboratoire de Physique Théorique et Hautes Energies, Univ. Paris VI, September 1973.

7) W. Männer, New results in ππ scattering, Paper presented at the 4th Internat. Conf. on Experimental Meson Spectroscopy, Boston, Mass., USA, 1974.

8) W. Ochs and F. Wagner, Phys. Letters 44B, 271 (1973).

9) S. Humble, Nuclear Phys. B98, 267 (1975).

Table 1

Results of the fits for the I = 2 phase shifts δ_s and δ_d

Mass interval (GeV)	δ_s^2 (deg)		δ_d^2 (deg)	
	Method A	Method B	Method A	Method B
0.3-0.4	-3.78 ± 1.72	-6.01 ± 0.45	-0.06 ± 0.04	-0.01 ± 0.01
0.4-0.5	-8.02 ± 1.15	-8.59 ± 0.34	-0.06 ± 0.03	-0.14 ± 0.03
0.5 0.6	-9.91 ± 1.26	-10.92 ± 0.34	-0.39 ± 0.22	-0.40 ± 0.05
0.6-0.7	-13.41 ± 1.55	-14.44 ± 0.49	-0.14 ± 0.06	-0.57 ± 0.08
0.7-0.8	-14.59 ± 1.60	-16.33 ± 0.56	-0.86 ± 0.35	-0.95 ± 0.11
0.8-0.9	-15.81 ± 2.06	-17.36 ± 0.62	-2.38 ± 0.43	-1.23 ± 0.12
0.9-1.0	-20.57 ± 2.06	-22.11 ± 0.78	-1.89 ± 0.44	-1.59 ± 0.16
1.0-1.1	-22.46 ± 2.64	-24.81 ± 1.03	-3.01 ± 0.50	-2.19 ± 0.21
1.1-1.2	-23.66 ± 2.52	-26.51 ± 1.03	-2.20 ± 0.52	-1.97 ± 0.23
1.2-1.3	-26.76 ± 3.15	-29.47 ± 1.24	-3.72 ± 0.63	-2.44 ± 0.33
1.3-1.4	-30.31 ± 3.55	-32.57 ± 1.67	-2.85 ± 0.37	-2.87 ± 0.38
1.4-1.5	-28.19 ± 5.30	-32.03 ± 1.89	-3.17 ± 1.12	-3.08 ± 0.47

Figure captions

Fig. 1 : Missing-mass distribution for the events identified as $\pi^+p \to \pi^+\pi^+ \ldots$ with (dotted area) and without (solid curve) the condition that none of the anticounters have fired.

Fig. 2 : $\pi^+\pi^+$ invariant mass spectrum for $\pi^+p \to \pi^+\pi^+n$ at 12.5 GeV. The solid line shows the number of events actually observed. The error bars indicate the number of events after correction for acceptance losses.

Fig. 3 : Spherical harmonic moments in the t-channel helicity frame of $\pi^+\pi^+$ in the reaction $\pi^+p \to \pi^+\pi^+n$ versus $\pi^+\pi^+$ invariant mass for events in the t-interval $-t_{min} < -t < 0.2$ GeV^2.

Fig. 4 : Normalized spherical harmonic moments $\langle \mathrm{Re}\, Y_\ell^m \rangle$ in both the t-channel and s-channel helicity frames of $\pi^+\pi^+$, in the reaction $\pi^+p \to \pi^+\pi^+n$, versus $\sqrt{-t}$ for events in the mass interval 0.75-1.25 GeV. The lines correspond to the values obtained from our amplitudes (12) using the parameters listed in Table 1.

Fig. 5 : Differential cross-section for events in the mass intervals 0.75-1.25 GeV (small dots) and 0.35-0.75 GeV (big dots).

Fig. 6 : Phase shifts δ_s, δ_d, and slope parameter B obtained from fits to our data with the amplitudes (12) as a function of $M_{\pi\pi}$. The solid lines in the δ_s and δ_d plots represent the dispersion relation predictions of Basdevant et al.[6].

Fig. 7 : Mass dependence in the interval $0.5 < M_{\pi\pi} < 1.5$ GeV of the parameter c obtained from the fits to our data using Eq. (12) (black dots), as determined from Eq. (13) (open circles), and the mass dependence that follows from Eq. (14) and the exponential slope B (approximated here by a smooth function) (drawn curve).

Fig. 8 : Ratio of the t-channel moments $\langle Y_2^0 \rangle$ and $\langle \mathrm{Re}\, Y_2^1 \rangle$ integrated over $-t_{min} < -t < 0.2$ GeV^2 in this experiment (black dots). For comparison the results obtained for the reaction $\pi^-p \to \pi^-\pi^+n$ [1] are shown (×).

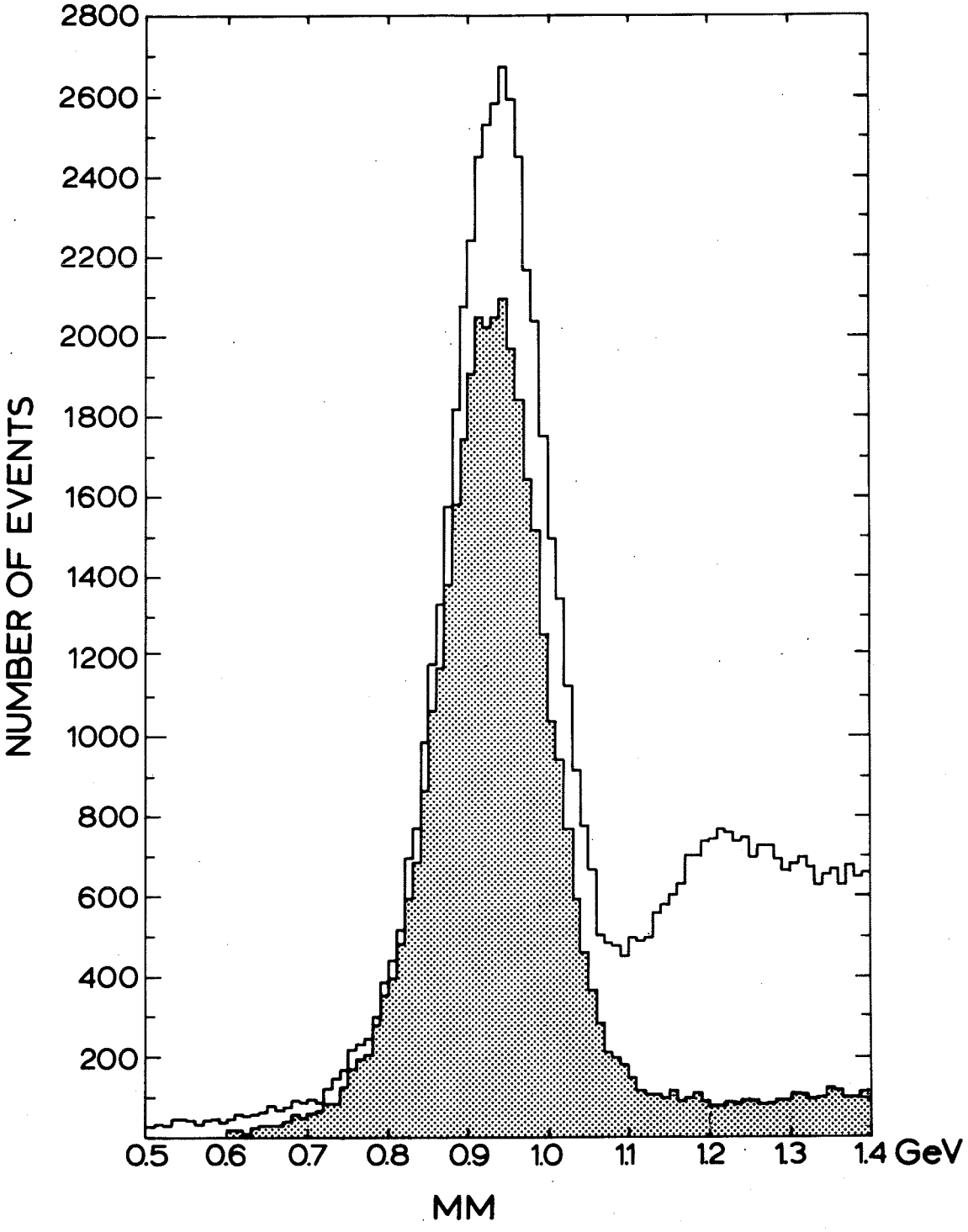
NUMBER OF EVENTS
2800
2600
2400
2200
2000
1800
1600
1400
1200
1000
800
600
400
200
0.5
0.6
0.7
0.8
0.9
1.0
1.1
1.2
1.3
1.4 GeV
MM

Fig. 1

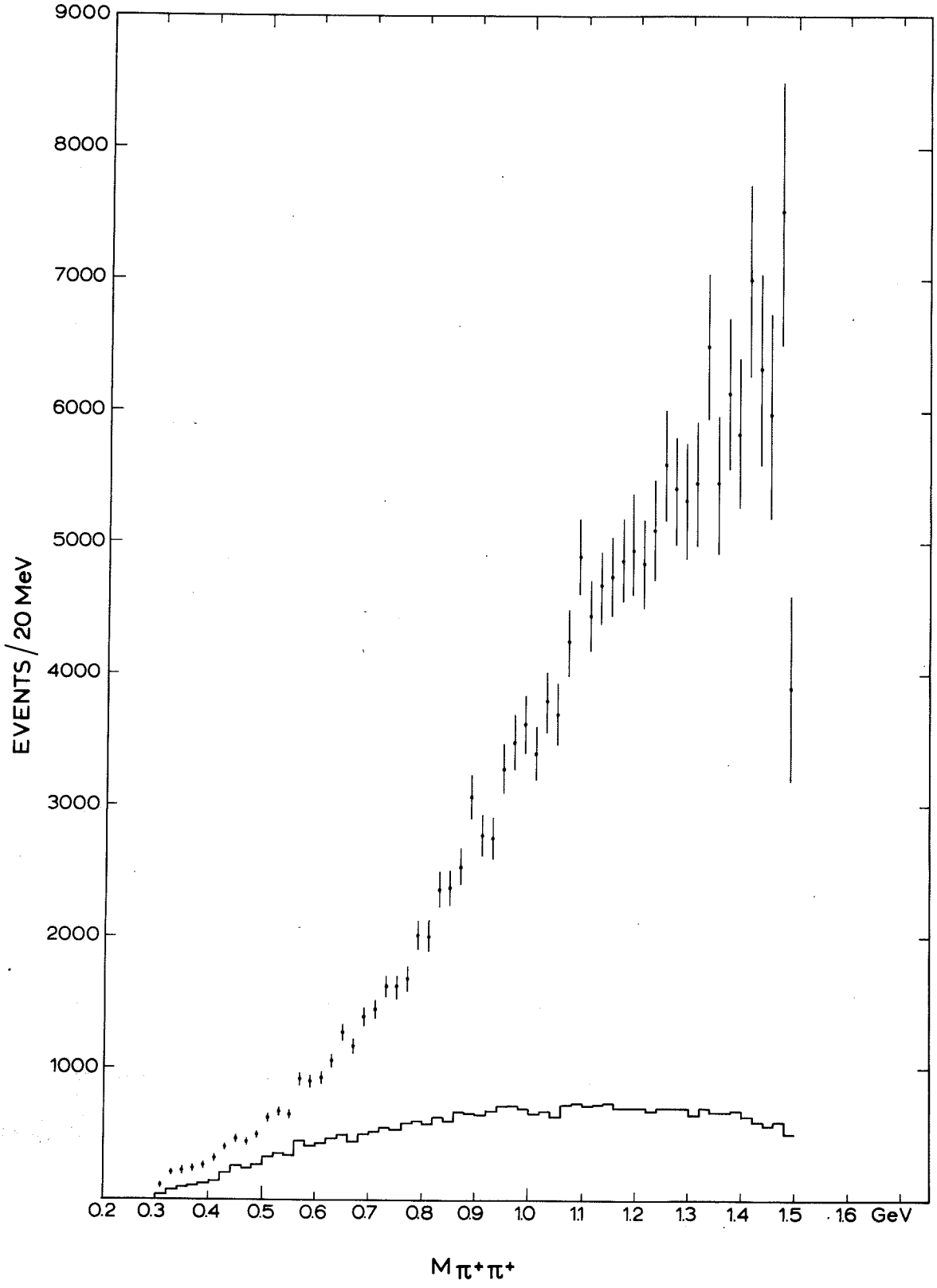
9000
8000
7000
6000
5000
4000
3000
2000
1000
EVENTS / 20 MeV
0.2
0.3
0.4
0.5
0.6
0.7
0.8
0.9
1.0
1.1
1.2
1.3
1.4
1.5
1.6 GeV
M π⁺π⁺

Fig. 2

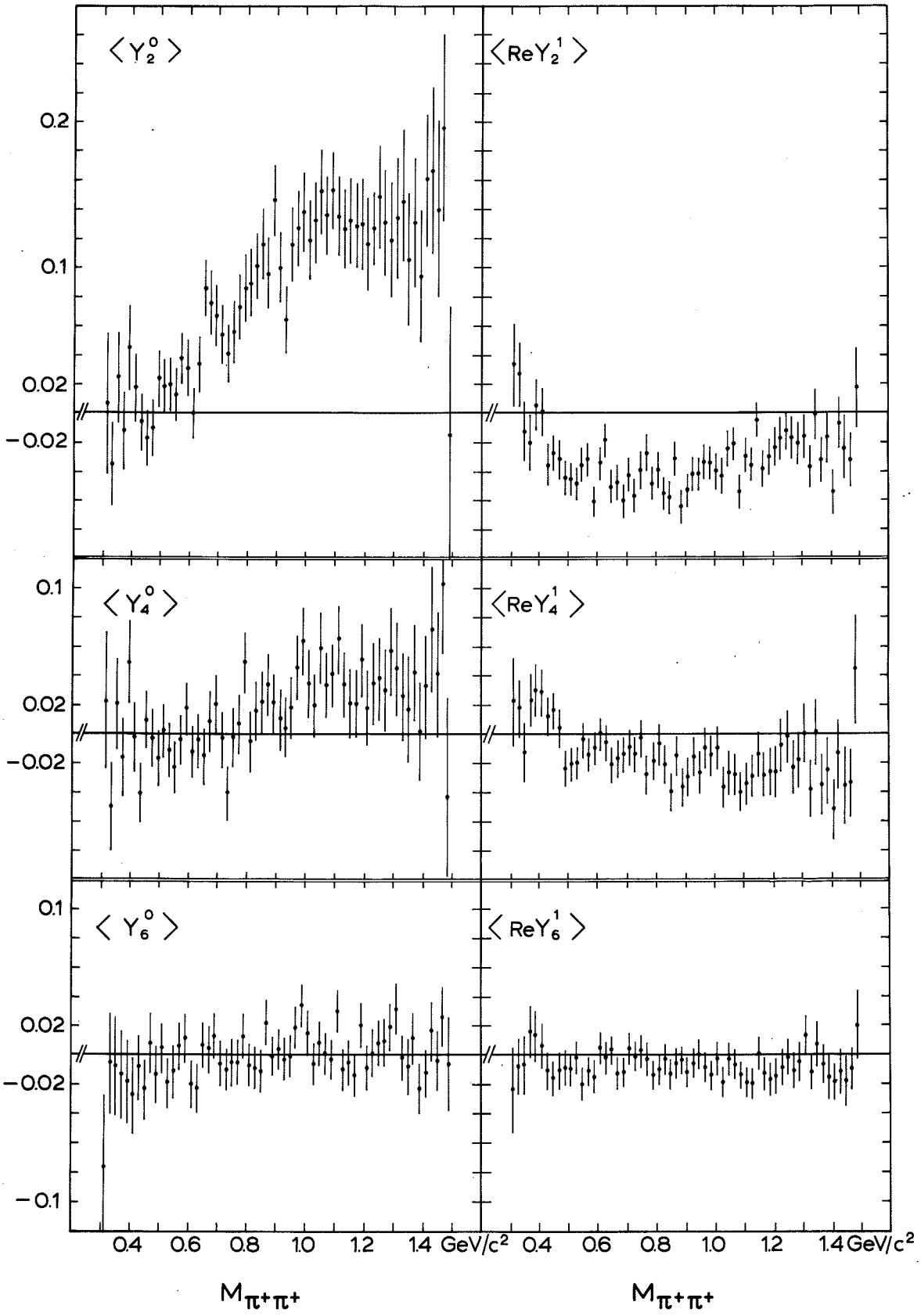
⟨ Y₂⁰ ⟩
⟨ ReY₂¹ ⟩
⟨ Y₄⁰ ⟩
⟨ ReY₄¹ ⟩
⟨ Y₆⁰ ⟩
⟨ ReY₆¹ ⟩
0.2
0.1
0.02
−0.02
0.1
0.02
−0.02
0.1
0.02
−0.02
−0.1
0.4 0.6 0.8 1.0 1.2 1.4 GeV/c²
0.4 0.6 0.8 1.0 1.2 1.4 GeV/c²
Mπ⁺π⁺
Mπ⁺π⁺

Fig. 3

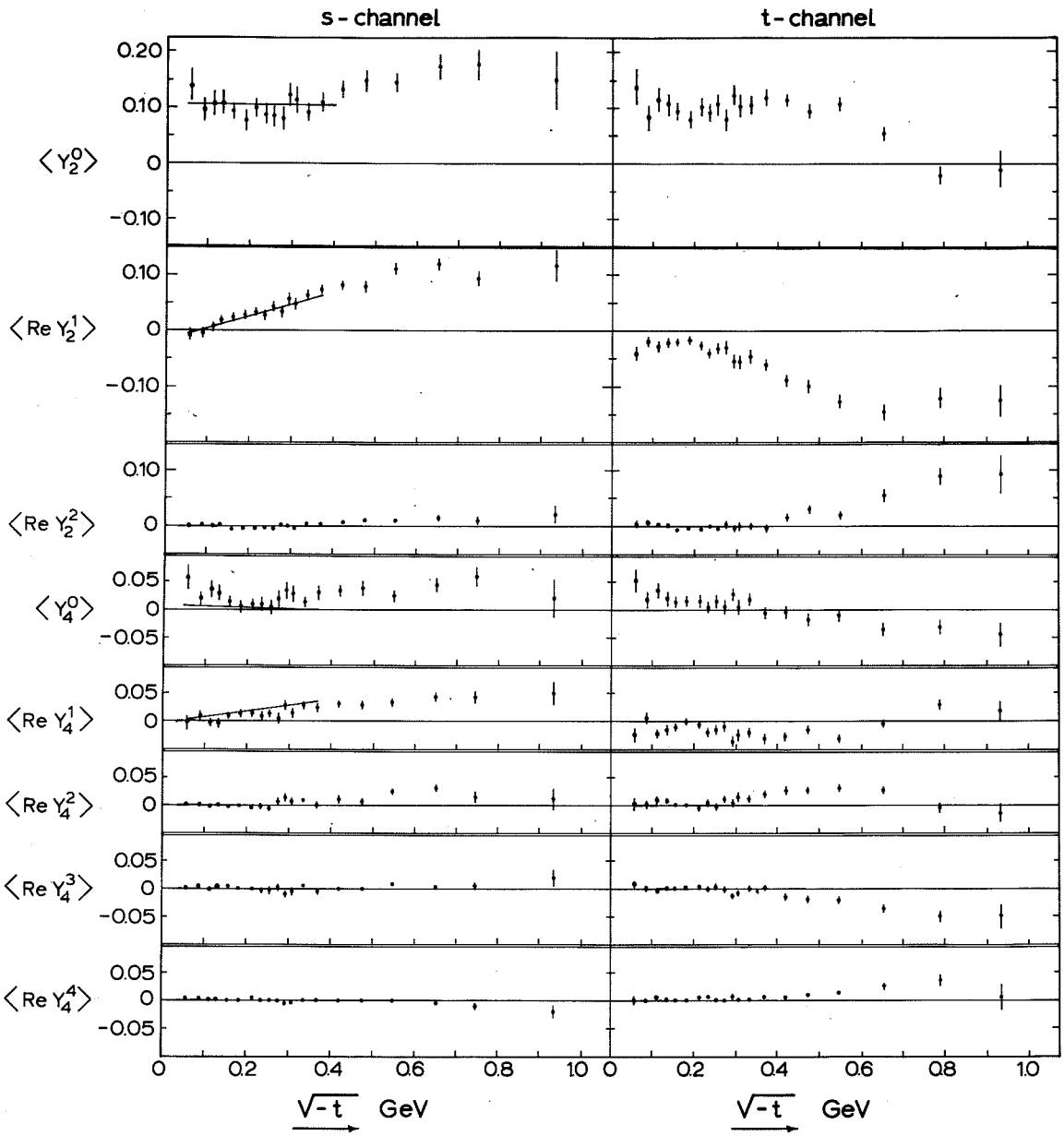
s - channel
t - channel
$\langle Y_2^0 \rangle$
$\langle \mathrm{Re}\, Y_2^1 \rangle$
$\langle \mathrm{Re}\, Y_2^2 \rangle$
$\langle Y_4^0 \rangle$
$\langle \mathrm{Re}\, Y_4^1 \rangle$
$\langle \mathrm{Re}\, Y_4^2 \rangle$
$\langle \mathrm{Re}\, Y_4^3 \rangle$
$\langle \mathrm{Re}\, Y_4^4 \rangle$
0.20
0.10
0
-0.10
0.05
-0.05
0.2
0.4
0.6
0.8
1.0
$\sqrt{-t}$ GeV

Fig. 4

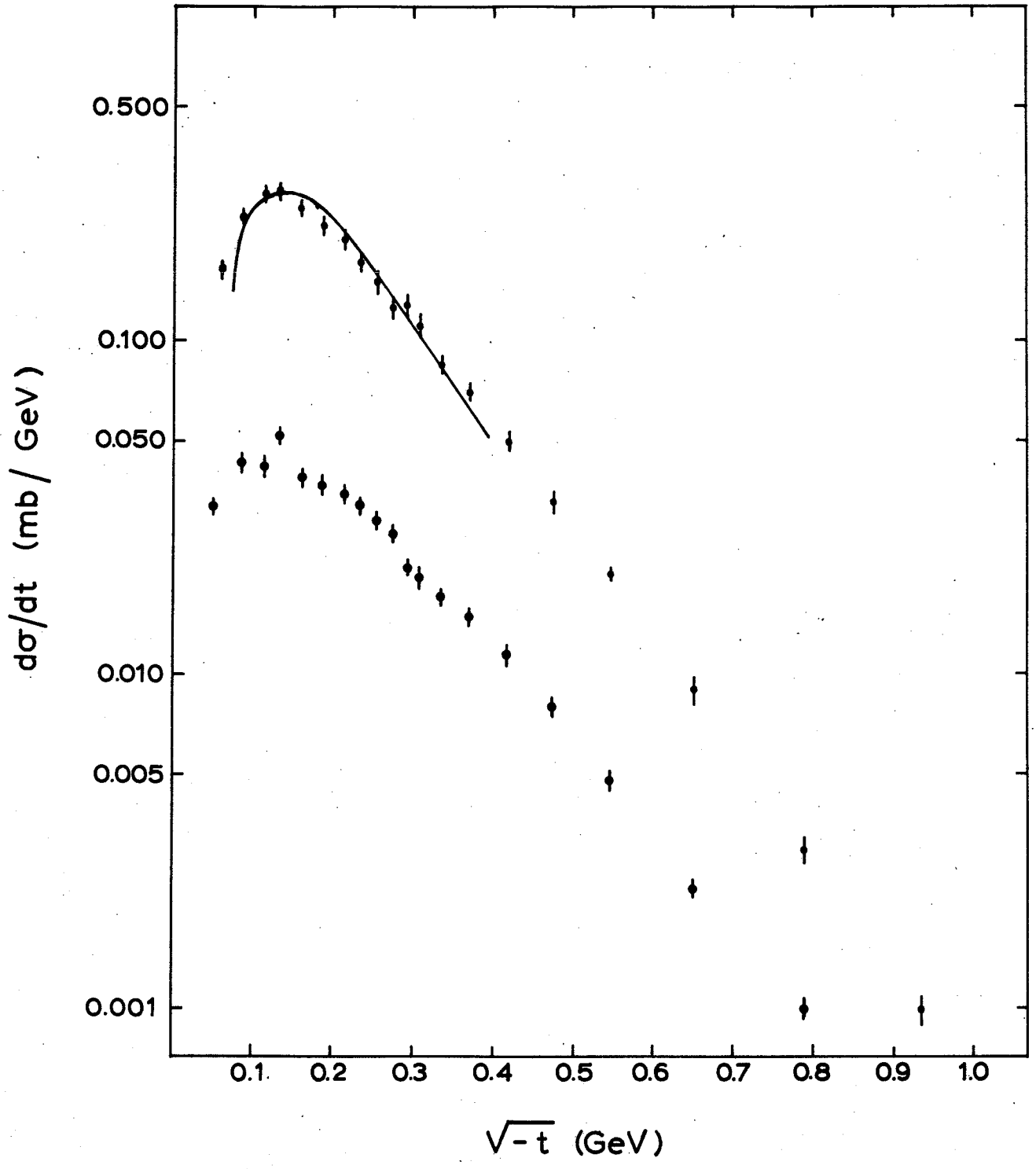
0.500
0.100
0.050
0.010
0.005
0.001
dσ/dt (mb / GeV)
0.1
0.2
0.3
0.4
0.5
0.6
0.7
0.8
0.9
1.0
√-t (GeV)

Fig. 5

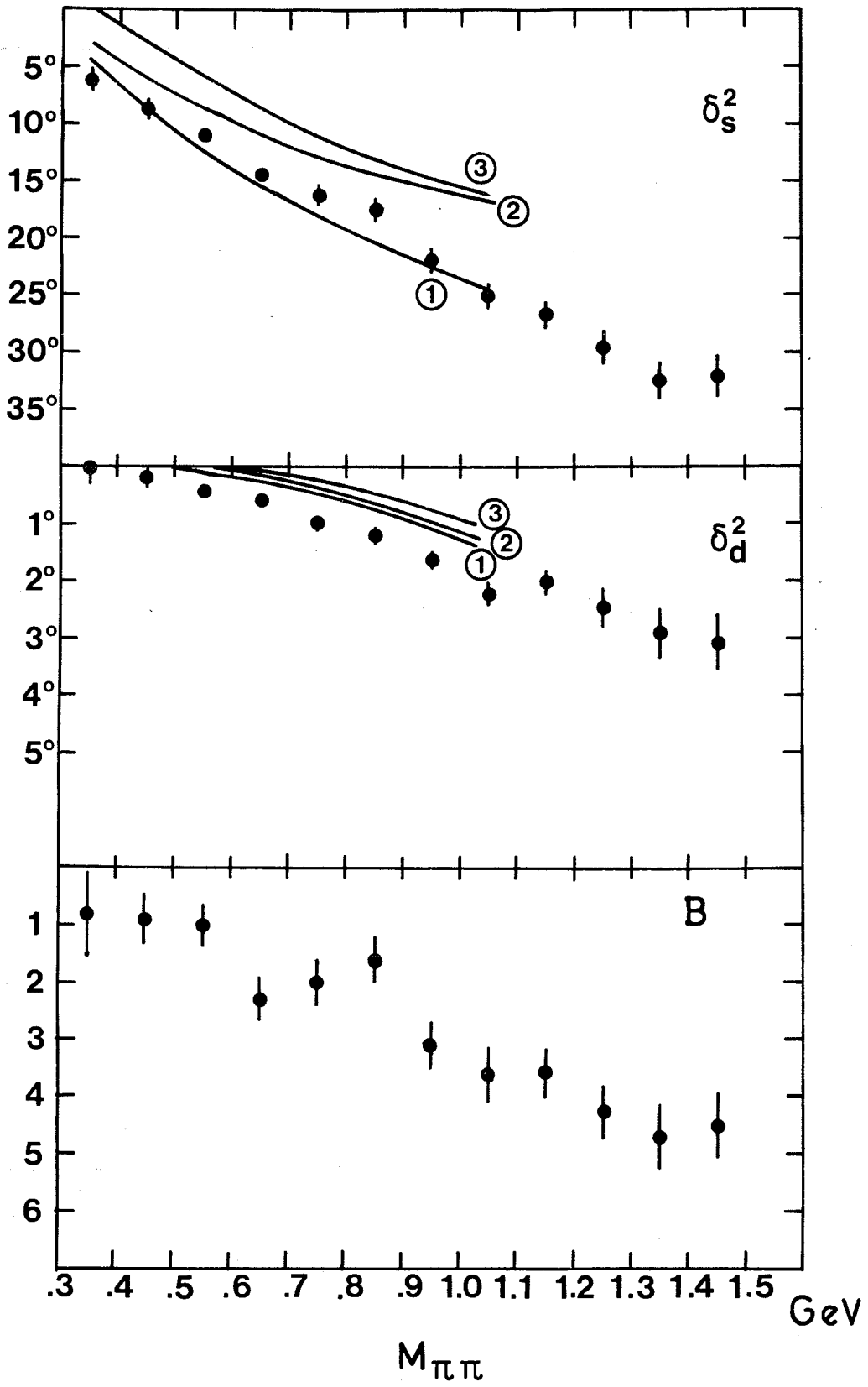
5°
10°
15°
20°
25°
30°
35°
δ_s^2
③
②
①
1°
2°
3°
4°
5°
δ_d^2
③
②
①
1
2
3
4
5
6
B
.3 .4 .5 .6 .7 .8 .9 1.0 1.1 1.2 1.3 1.4 1.5
GeV
$M_{\pi\pi}$

Fig. 6

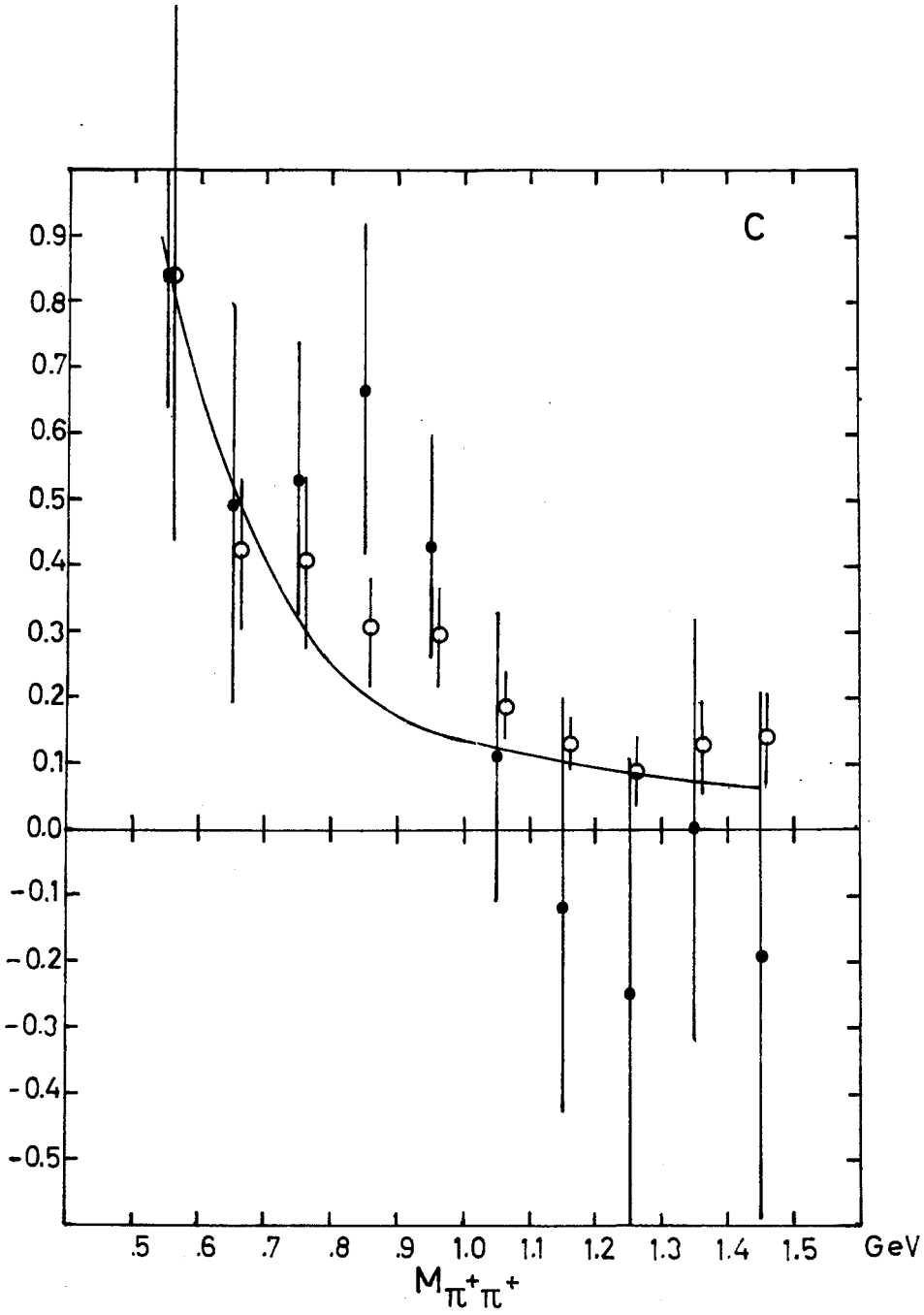
C
0.9
0.8
0.7
0.6
0.5
0.4
0.3
0.2
0.1
0.0
-0.1
-0.2
-0.3
-0.4
-0.5
.5
.6
.7
.8
.9
1.0
1.1
1.2
1.3
1.4
1.5
GeV
$M_{\pi^+\pi^+}$

Fig. 7

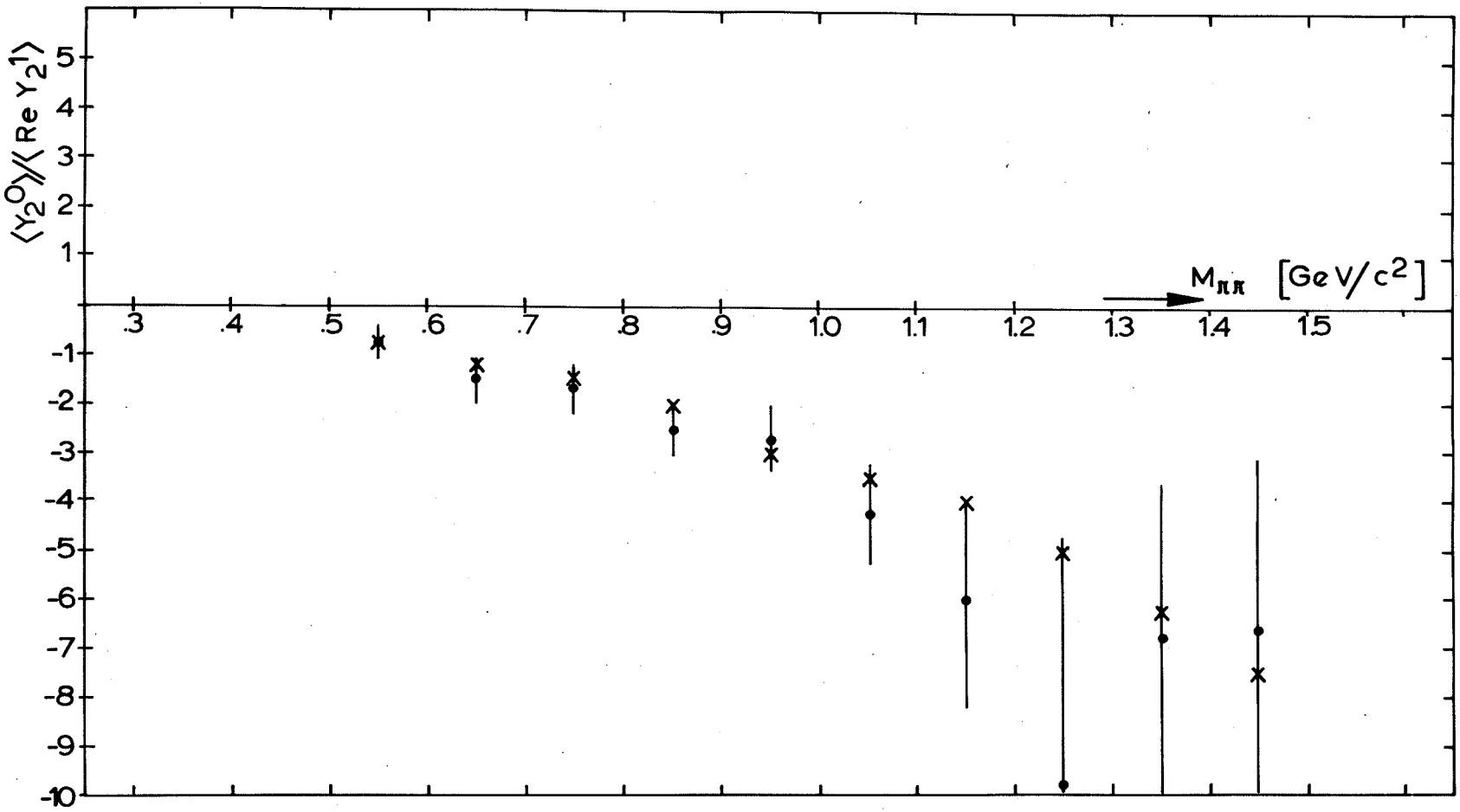
$\langle Y_2^0 \rangle / \langle \mathrm{Re}\, Y_2^1 \rangle$
5
4
3
2
1
-1
-2
-3
-4
-5
-6
-7
-8
-9
-10
.3
.4
.5
.6
.7
.8
.9
1.0
1.1
1.2
1.3
1.4
1.5
$M_{\pi\pi}$ [GeV/c^2]

Fig. 8